

Title	Growth of crystalline copper silicide nanowires in high yield within a high boiling point solvent system
Authors	Geaney, Hugh; Dickinson, Calum; O'Dwyer, Colm; Mullane, Emma; Singh, Ajay; Ryan, Kevin M.
Publication date	2012-10-29
Original Citation	Geaney, H., Dickinson, C., O'Dwyer, C., Mullane, E., Singh, A. and Ryan, K. M. (2012) 'Growth of Crystalline Copper Silicide Nanowires in High Yield within a High Boiling Point Solvent System', Chemistry of Materials, 24(22), pp. 4319-4325. doi: 10.1021/cm302066n
Type of publication	Article (peer-reviewed)
Link to publisher's version	<a href="https://pubs.acs.org/doi/abs/10.1021/cm302066n">https://pubs.acs.org/doi/abs/10.1021/cm302066n</a> - 10.1021/cm302066n
Rights	© 2012 American Chemical Society. This document is the Accepted Manuscript version of a Published Work that appeared in final form in Chemistry of Materials, copyright © American Chemical Society after peer review and technical editing by the publisher. To access the final edited and published work see <a href="https://pubs.acs.org/doi/abs/10.1021/cm302066n">https://pubs.acs.org/doi/abs/10.1021/cm302066n</a>
Download date	2024-04-10 17:33:31
Item downloaded from	<a href="https://hdl.handle.net/10468/6283">https://hdl.handle.net/10468/6283</a>



**UCC**

**University College Cork, Ireland**  
Coláiste na hOllscoile Corcaigh

# Growth of Crystalline Copper Silicide Nanowires in High Yield within a High Boiling Point Solvent System

*Hugh Geaney<sup>1,2</sup>, Calum Dickinson,<sup>1</sup> Colm O Dwyer,<sup>1,4,5</sup> Emma Mullane,<sup>1,2</sup> Ajay Singh,<sup>1,2,3</sup> Kevin M. Ryan<sup>1,2,3\*</sup>*

<sup>1</sup>Materials and Surface Science Institute and Department of Chemical and Environmental Sciences,  
University of Limerick, Limerick, Ireland

<sup>2</sup> Department of Chemical and Environmental Sciences, University of Limerick

<sup>3</sup> SFI-Strategic Research Cluster in Solar Energy Research, University of Limerick, Limerick,  
Ireland

<sup>4</sup> Department of Chemistry, University College Cork, Cork, Ireland

<sup>5</sup> Tyndall National Institute, Lee Maltings, Cork, Ireland

\*To whom correspondence should be addressed. Email: **Kevin.M.Ryan@ul.ie**

## RECEIVED DATE

## Abstract

Here, we report the formation of high density arrays of Cu<sub>15</sub>Si<sub>4</sub> nanowires using a high boiling point organic solvent based method. The reactions were carried out using Cu foil substrates as the Cu source with nanowire growth dependent upon the prior formation of Cu<sub>15</sub>Si<sub>4</sub> crystallites on the surface. The method shows that simple Si delivery to metal foil can be used to grow high densities of silicide nanowires with a tight diameter spread at reaction temperatures of 460 °C. The nanowires are characterized by HRTEM, HRSEM, XPS and show low resistivities, while coupling capacity and unit impedance were also determined through electrical analysis.

**Keywords: silicide nanowires, copper, high boiling point solvent synthesis**

## **Introduction**

Metal silicides are an important material set with a multitude of phases stable, from metal to Si rich, allowing for functional property variation according to their respective stoichiometric ratios. Their inherent compatibility with silicon makes them particularly suitable for a range of semiconductor applications from contact junctions to gate materials.<sup>1</sup> Discrete metal silicides in nanowire (NW) form are gaining increasing interest for interconnect applications, where low resistivities combined with a stable crystal structure may offer an attractive alternative to pure metal. To date, a variety of metal silicide NWs have been formed including NiSi,<sup>2</sup> FeSi<sup>3</sup> and CoSi<sup>4</sup>. The diffusivity of the metal in Si, is the strongest driving force for silicide formation with Ni showing high diffusivity resulting in a wide range of stoichiometries with six different phases successfully reported.<sup>5-7</sup> Synthesis protocols for Ni silicide NWs have included metal evaporation onto Si NW followed by annealing<sup>8</sup>, the co-delivery of metal and Si atoms to substrates,<sup>9-11</sup> or the reaction of a Si precursor with metal foil.<sup>12</sup> Nanowire formation with metal silicides is complicated by the preponderance of metal silicide nanoparticles in themselves to function as seeds for single crystal growth of Si NWs by vapor solid solid (VSS) protocols.<sup>13</sup> Therefore, obtaining one dimensional metal silicide nanostructures inherently demands controlled delivery of both metal and Si to the NW growth zone in a process which does not favour pure Si NW growth. This has limited the range and type of metal silicide NWs that can be successfully formed.

Cu silicides in particular are an extremely promising material set which in thin-film form have found uses as Cu ion diffusion barriers and as passivation layers for on chip applications.<sup>14,15</sup> In nanocrystal morphologies, the predominant phase reported to date has been Cu<sub>3</sub>Si, with nanotriangles, nanosquares and nanorods formed by Cu powder evaporation with and without the presence of an Au catalyst.<sup>16,17</sup> Freestanding Cu<sub>3</sub>Si NWs with diameters between 200 and 300 nm have also very recently

been formed using a Ge catalyzed method.<sup>18</sup> While polycrystalline Cu silicides with higher stoichiometric ratio of metal have been formed at the nanoscale,<sup>19</sup> the growth of single crystal NW which are rich in Cu may be of considered interest due to the possibility of even lower resistivities in a single crystal NW.<sup>1</sup> Cu silicides would be well placed as interconnect materials due to the high abundance and ubiquity of Cu within microelectronics processing and the potential for Cu diffusion suppression through the use of Cu silicides rather than pure Cu.<sup>20</sup>

Here we present the growth of  $\text{Cu}_{15}\text{Si}_4$  NWs through the delivery of Si to bulk copper foil using a simple glassware based approach. The Si flux required for growth was formed by thermally decomposing phenylsilane (PS) in a high boiling point organic solvent (HBS) medium.<sup>21</sup> Initially, a non-uniform thin film of  $\text{Cu}_{15}\text{Si}_4$  is formed on the copper surface consisting of large micron size crystalline grains. Once the metal surface is covered, the preferred  $\text{Cu}_{15}\text{Si}_4$  crystal habit changes from large micron size grains to anisotropic NWs with diameters of the order of 100 nm. The NW growth directions are compatible with the underlying crystal resulting in either single NWs or multipod (di-, tri- and tetra-pod) structures with the underlying crystal as the seed. The lengths of the NWs are experimentally tunable according to the growth time with structural and electrical characterisation confirming single crystal growth (primarily in the  $\langle 111 \rangle$  direction) with resistivities of the order of  $\sim 208 \mu\Omega \text{ cm}$ .

## **Experimental:**

### **Substrate preparation and reaction setup**

Cu foil was purchased from Goodfellows with a 0.25 mm thickness and 99.9 % purity. The Cu was cleaned with 0.1 M nitric acid and rinsed repeatedly with deionized water and then dried before introduction into the reactor setup. After reaction, the NW covered substrates were removed from the reaction flask. The substrates were rinsed with toluene to remove residual high boiling point solvent (HBS) and dried under a  $\text{N}_2$  line prior to characterization.

Reactions were carried out in custom made Pyrex, round bottomed flasks using 7ml of Squalane (99% Aldrich). The Cu growth substrates were placed vertically in the flask which was attached to a Schlenk line setup via a water condenser. This was then ramped to a temperature of 125 °C using a three zone furnace. A vacuum, of at least 100 mTorr, was applied for 1 hour to remove moisture from the system. Following this, the system was purged with Ar. The flask was then ramped to the reaction temperature. Reactions were conducted at 460 °C. Upon reaching the reaction temperature, 0.5 ml ( $4.06 \times 10^{-3}$  moles) phenylsilane (PS) was injected through a septum cap. Thermal decomposition of the phenylsilane proceeds via established phenyl redistribution pathways to provide the Si monomer for NW growth.<sup>21,22</sup> Reaction times between 10 minutes and 90 minutes were investigated. To terminate the reaction, the furnace was turned off and the setup was allowed to cool to room temperature before extracting the NW coated substrates.

For comparison, reactions were also carried out using a 20 nm thick Cu layer evaporated on stainless steel. The stainless steel was found to be non reactive at the temperatures investigated. A 30 minute reaction time was probed using  $4.06 \times 10^{-3}$  moles of PS. All other parameters and reactions were as above.

## Analysis

SEM analysis was performed on a Hitachi SU-70 system operating between 3 and 20 kV. The Cu substrates were untreated prior to SEM analysis. For TEM analysis, the NWs were removed from the growth substrates through the use of a sonic bath. TEM analysis was conducted using a 200 kV JEOL JEM-2100F field emission microscope equipped with a Gatan Ultrascan CCD camera and EDAX Genesis EDS detector. EDX analysis of the NWs was conducted on Au TEM grids. XRD analysis was conducted using a PANalytical X'Pert PRO MRD instrument with a Cu-K $\alpha$  radiation source ( $\lambda = 1.5418$  Å) and an X'celerator detector. XPS was performed in a Kratos AXIS 165 spectrometer using monochromatic Al K $\alpha$  radiation of energy 1486.6 eV. High resolution spectra were

taken at fixed pass energy of 20 eV. Binding energies were determined using C 1s peak at 284.8 eV as charge reference. For construction and fitting of synthetic peaks of high resolution spectra, a mixed Gaussian-Lorentzian function with a Shirley type background subtraction were used.

Electrical analysis of the Cu<sub>15</sub>Si<sub>4</sub> NWs was carried out by drop-casting a solution of the NWs directly onto Au electrodes with external contact pads. Charge transport measurements for the Cu silicide NWs were conducted using 2-probe measurements with a dc-voltage and an Agilent 34401A Digital Multimeter in a Peltier cell, thermostated to 295 K in a Faraday cage. Liquid metal contacts were made using In-Ga eutectic blown into a sphere from a gold metallized short borosilicate capillary tube ensuring good wetting (several  $\mu\text{m}^2$ ) to the gold contact pads of the patterned electrode. NW resistance and contact resistivity values were extracted from  $I$ - $V$  curves.

## **Results and Discussion:**

In a typical experiment, the reaction of PS on copper foil for 30 minutes within the HBS growth system results in dense NW formation across large areas (see Figure 1 a). HBS vapour has recently been highlighted as a flexible medium for attaining the high nucleation temperatures required for the formation Si and Ge NWs.<sup>23-26</sup> The NWs here have an average diameter of 108 nm with a standard deviation of 9 nm and are untapered along their lengths (Figure S1 supporting information). The substrates post synthesis were a grey/brown colour and were obviously altered from the starting Cu foil substrates (Figure S2 supporting information).

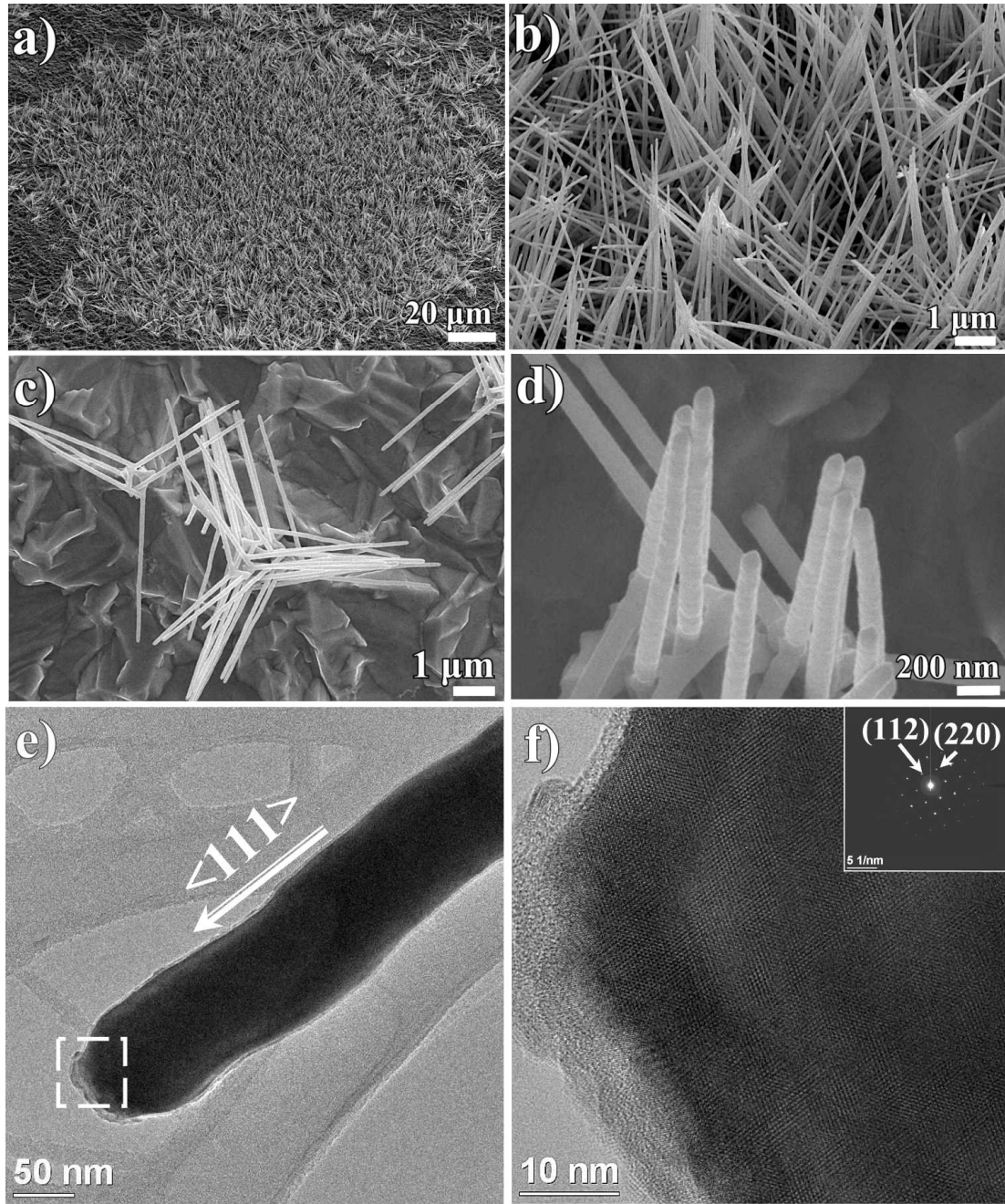


**Figure 1:** a) SEM image showing the large area coverage of the  $\text{Cu}_{15}\text{Si}_4$  NWs. b) Higher magnification image of the NWs showing the consistent NW diameters. c) SEM image showing an area of lower NW density and the underlying substrate material. d) SEM image of the slightly undulating surface of the NWs. e,f) TEM analysis of a single  $\text{Cu}_{15}\text{Si}_4$  NW. e) low magnification image of the NW with  $\langle 111 \rangle$  growth direction marked on the NW. The inset area is magnified in the HRTEM image in f) showing the crystallinity of the NW. The inset selected area electron diffraction pattern (viewed down the  $[110]$  zone axis) is indexed for the cubic  $\text{Cu}_{15}\text{Si}_4$  phase

In areas of more sporadic NW coverage, the growth of the NWs from the underlying substrate could be more easily examined. In Figure 1 c) it can be seen that the NWs are growing from the underlying crystalline material at defined angles. The growth is reminiscent of tetrapods which have been observed in a number of nanocrystal systems (see Supporting Information Figure S3 for TEM).<sup>27-</sup>  
<sup>29</sup> In Figure 1 d) the higher magnification SEM image was taken at a 70 tilt angle and shows the slightly rough surface of the NWs. The low resolution TEM image in Figure 1 e) shows a single NW with a diameter of approximately 98 nm growing in the  $\langle 111 \rangle$  direction. A HRTEM image taken from the marked area in e) is shown in f). A circa 3 nm amorphous coating can be seen at the extremity of the NW with the 2-D lattice fringes of the crystalline NW clearly evident. The inset selected area electron diffraction pattern (viewed down the  $[110]$  zone axis) is indexed with spots which correspond to the spacings for  $\text{Cu}_{15}\text{Si}_4$  with space group I-43d (see Supporting Information Figure S4 for fully indexed pattern). The indexed pattern further confirmed the  $\langle 111 \rangle$  growth direction. The majority of the NWs formed by this method were found to possess  $\langle 111 \rangle$  growth directions while a portion ( $\approx 20\%$ ) exhibited  $\langle 112 \rangle$  growth directions (Supporting information Figure S5).

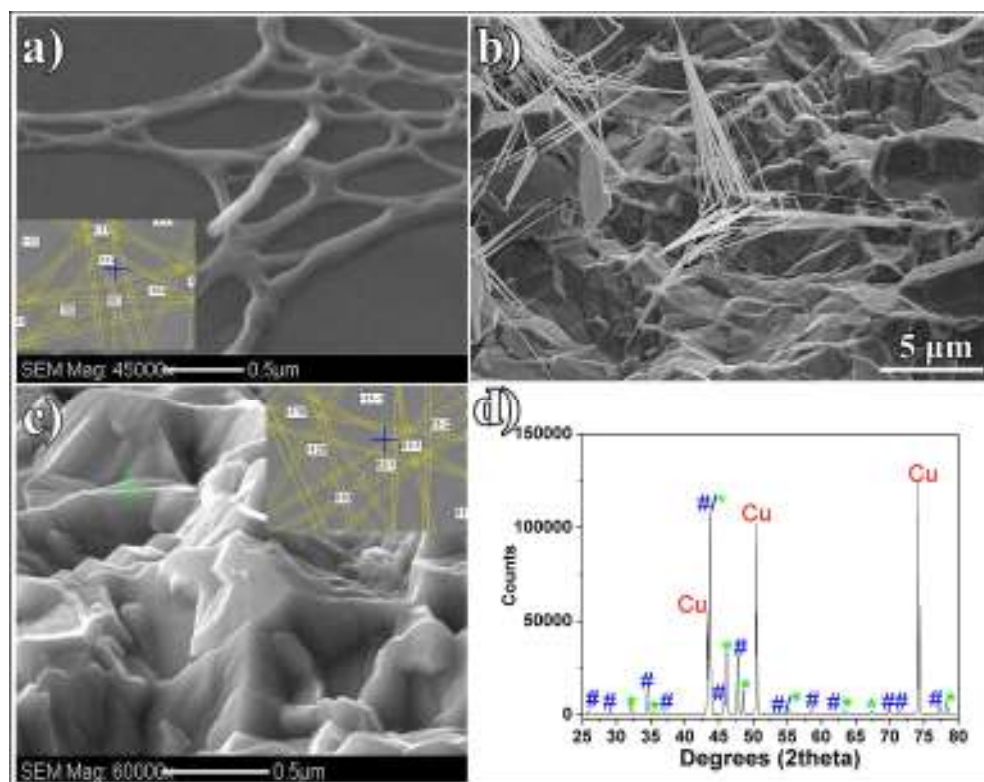


**Figure 2:** SEM image of a  $\text{Cu}_{15}\text{Si}_4$  NW taken on an lacey carbon TEM grid with inset EBSD pattern indexed for the cubic  $\text{Cu}_{15}\text{Si}_4$  phase. b) Illustration of the  $\text{Cu}_{15}\text{Si}_4$  NWs grown from the underlying crystallites. c) SEM of a portion of the underlying crystalline material with inset EBSD analysis again indicating the  $\text{Cu}_{15}\text{Si}_4$  phase. d) XRD pattern taken from a NW covered substrate with the marked reflections corresponding to #  $\text{Cu}_{15}\text{Si}_4$  \* $\text{Cu}_{0.83}\text{Si}_{0.17}$  and Cu.

In Figure 2 a), an individual NW across the supporting carbon lace is further analysed. The inset EBSD pattern is again consistent with that expected for cubic  $\text{Cu}_{15}\text{Si}_4$  with space group I-43d. All the NWs analyzed using this technique indicated that this phase was exclusively present in the sample (see Supporting Information S6 for additional examples and unindexed patterns). The SEM image in Figure 2 b) was taken at a 70 ° tilt and gives a clearer illustration of the faceted substrate material from which the NWs were grown. This appearance of crystallites across the substrate surface was visibly different from the pristine Cu observed prior to the reaction (Supporting Information S7). Separate EBSD analysis of the substrate (Figure 2 c)) also gave patterns consistent with the  $\text{Cu}_{15}\text{Si}_4$  phase. XRD analysis (Figure 2 d)) of the NW covered substrate confirmed the presence of  $\text{Cu}_{15}\text{Si}_4$  (indexed with a #). However additional reflections consistent with the presence of  $\text{Cu}_{0.83}\text{Si}_{0.17}$  (indexed with a \*) and

Cu were also observed. The absence of this phase from EBSD analysis suggests that this copper rich phase lies between the copper metal and the crystallite layer of  $\text{Cu}_{15}\text{Si}_4$ . The appearance of the additional Cu silicide phase underneath is unsurprising given the complex nature of the Cu/Si phase diagram<sup>30</sup> and also the variety of phases which have been found to exist for other transition metal silicides.<sup>31-33</sup> Furthermore, it has previously been shown that upon annealing, Cu silicide phases will tend to form Cu rich phases by a Si diffusion based reaction.<sup>34</sup>

The nature of the Cu/Si phase diagram is complex with a variety of phases possible.<sup>30</sup> The majority of reports to date studying Cu silicides have presented the formation of the orthorhombic  $\text{Cu}_3\text{Si}$   $\eta''$  phase rather than the other low temperature equilibrium phases  $\text{Cu}_{15}\text{Si}_4$  and  $\text{Cu}_5\text{Si}$ .<sup>18,35</sup> Previously, the formation of higher Cu ratio silicides has required reaction temperatures of greater than 525 K and the presence of excess Cu.<sup>35</sup> The formation of the  $\text{Cu}_{15}\text{Si}_4$  phase here may thus be due to these two conditions being satisfied. In the case of the Ge NWs previously grown in our system from Cu foil, the intermediate Cu germanide phase formed on top of the cubic Cu foil was  $\text{Cu}_3\text{Ge}$  (orthorhombic).<sup>24</sup> The Ge NWs (cubic) grew on top of the  $\text{Cu}_3\text{Ge}$  and it was found that the resultant  $\text{Cu}_3\text{Ge}$  catalyst seeds which remained on the NW tips post-synthesis were oriented such that the lattice spacing of the seed closely matched that of the  $\langle 110 \rangle$  growth directions of the Ge NWs. Similarly, previous reports using Cu as a seed for elemental Si NW formation have always led the formation of orthorhombic  $\text{Cu}_3\text{Si}$  catalyst seeds from the initial Cu nanoparticles.<sup>36-38</sup> It thus seems likely that pure Si NWs would have been formed in this system had  $\text{Cu}_3\text{Si}$  crystallites been formed on the Cu substrate rather than  $\text{Cu}_{15}\text{Si}_4$  crystallites. Therefore, the phase of silicide (or germanide) formed on the substrate plays an important role in determining whether pure Si (or Ge) NWs or silicide (germanide) NWs form.

The occurrence of the  $\text{Cu}_{15}\text{Si}_4$  phase both as a bulk crystallite and in NW form is interesting and suggests the NW crystal habit emerges from the underlying crystal under appropriate conditions. The occurrence of multipod geometries is not due to having a core of a different phase vis a vis II-VI tetrapods where a zinc-blende nucleus allows growth of wurtzite arms.<sup>39</sup> Here, the NWs emerge from

the available faces of the underlying crystal and it is likely that their angle is defined by the relationship between the NW growth directions and the underlying crystallites. Multiple NWs can emerge from the same face resulting in the densities of packing observed. The ability to form multipod structures is largely defined by the topography of the crystallite and number of unconstrained facets for the NW habit to emerge. Ge NWs (which also possess a cubic crystal structure) were previously shown to grow epitaxially with  $\langle 111 \rangle$  growth directions from underlying Ge microcrystals in a similar vein.<sup>40</sup>

XPS was performed to examine the chemistry of the copper silicide NWs. A low-resolution survey spectrum identified the presence of Cu, Si O and C. High resolution spectra of Cu 2p and Si 2p were measured to determine the chemical states of the elements. The Cu 2p spectrum (supporting information Figure S8a) appears as a narrow doublet peak with  $2p_{3/2}$  at 933.3 eV and  $2p_{1/2}$  at 953.2 eV. It is clear from the absence of satellite peaks that copper (II) oxide is not present. The peaks can be assigned to copper silicide or copper (I) oxide whose binding energies are very close.<sup>41-43</sup> However, due to evidence from the XRD and EBSD for silicidation and the narrow FWHM (full width at half maximum of peak) it is possible to assign the peak to a single compound of copper silicide. The high resolution Si 2p spectrum (supporting information Figure S8b) can be fitted with three sets of doublets. The narrow doublet peaks with  $2p_{3/2}$  at 99.6 eV can be assigned to silicide.<sup>42,43</sup> The two sets of doublets at higher binding energies 101.5 eV and 102.5 eV, also supported by the presence of O are indicative of surface oxidation of the silicide NWs and can be assigned to  $\text{Si-O}_x$  ( $x < 2$ ) and  $\text{SiO}_2$  respectively.

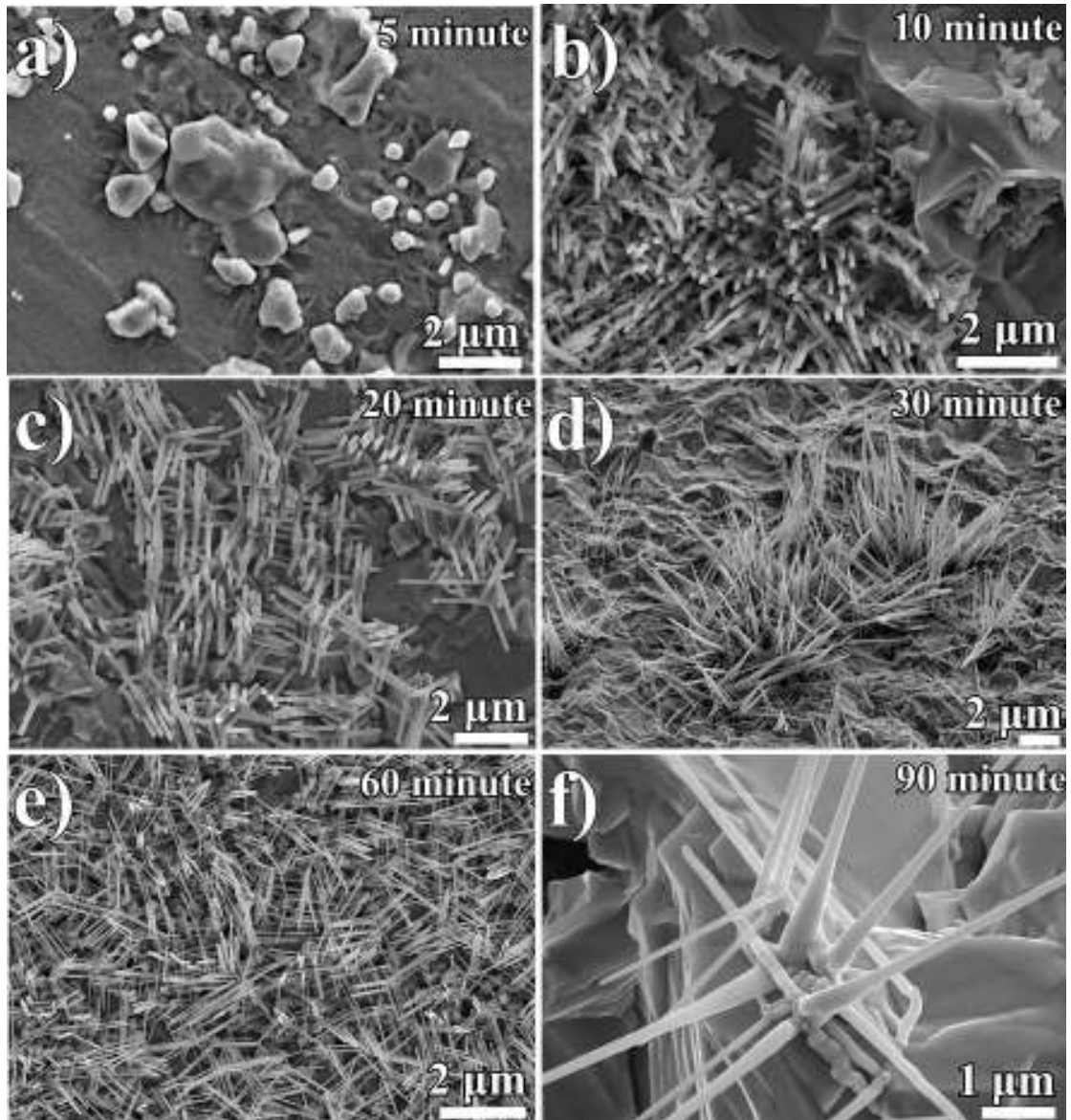


**Figure 3:** SEM images taken from a reaction time investigation. a) Isolated  $\text{Cu}_{15}\text{Si}_4$  crystallites formed on the underlying Cu substrate after 5 minutes. b) 10 minute reaction time leading to short NW growth ( $<1\ \mu\text{m}$  in length). c) 20 minute reaction time leading to increased NW length  $\approx 2\ \mu\text{m}$ . d) 30 minute reaction time leading to NWs with lengths  $\approx 5\ \mu\text{m}$ . e) Increased NW density after 1 hour reaction time. f) Evidence of radial growth at an extended reaction of 1.5 hr.

A full reaction time investigation was undertaken to assess its impact over NW morphology as shown in Figure 3. 5 minute reaction times led to the formation of isolated  $\text{Cu}_{15}\text{Si}_4$  crystallites on the underlying Cu (Figure 3 a)). The incremental control achievable over NW length by simply varying reaction time from 10 to 30 minutes can be seen in Figures 3 b)-d), where the average NW length can be altered from  $\approx 1\ \mu\text{m}$  to  $\approx 2\ \mu\text{m}$  and finally  $\approx 5\ \mu\text{m}$  (with no appreciable increase in NW diameter).

Further increasing the reaction time to 60 minutes simply led to an increased density of NWs with comparable lengths and diameters ( $\approx 5\ \mu\text{m}$  and just over 100 nm respectively) to those grown after 30 minutes (Figure 3 e)). Further extension of the reaction time led to radial growth at the base of the NWs, causing the formation of needle-like NWs with base diameters of 200 nm or more (Figure 3 f)). This suggests that such long dwell times favor increased radial growth for the NWs rather than further elongation axially.

To investigate the importance of Cu diffusion from the underlying Cu substrate in facilitating  $\text{Cu}_{15}\text{Si}_4$  NW growth, reactions were carried out using a 20 nm thick evaporated Cu layer on stainless steel (Supporting Information Figure S9). It was found that Cu silicide crystallites formed on the substrate, however, the lack of a continued Cu source via diffusion from the metal foil resulted in the formation of Cu silicide seeded Si NWs. This shows that after the initial Cu source on the substrate has been consumed in the formation of Cu silicide nanocrystals, additional Si vapour supply results in the formation of pure, elemental Si NWs with well faceted Cu silicide tips (indicating a VSS NW growth mechanism).<sup>26,44</sup>

When considering the growth mechanism for the  $\text{Cu}_{15}\text{Si}_4$  NWs in this report (depicted schematically Supporting Information Figure S10), there are noticeable parallels with the mechanisms proposed for the growth of the Ni silicide NWs.<sup>31,32</sup> There, the formation of Ni silicide crystallites was assumed to be a prerequisite for NW growth. Here, through the use of EBSD analysis, we have shown the NWs grow directly from crystallites of the same Cu silicide phase. The decomposition of PS within the vapour phase of the HBS allows the formation of  $\text{Cu}_{15}\text{Si}_4$  crystallites on the substrate from the reaction of the silane vapour with the Cu foil. Continued Si vapour supply then results in the formation of single crystalline NWs from nucleation sites on the crystallites, with the continued formation of Cu silicide NWs rather than elemental Si driven by continued Cu diffusion from the underlying Cu substrate (facilitated by the high diffusivity of Cu in Si).<sup>14</sup> The compositional homogeneity along the NWs (Supporting information Figure S11) as they grow from the underlying

silicide phase suggests that Cu is actively diffusing from the underlying substrate into the structures. This is further strengthened by the illustration here that reactions conducted using a thin Cu source layer result exclusively in the formation of Cu silicide catalyzed Si NWs.  $\text{Cu}_{15}\text{Si}_4$  crystallite formation on the underlying Cu substrate appears to proceed via a Stransky-Krastanov type growth,<sup>45</sup> with discrete island formation on top of on underlying  $\text{Cu}_{15}\text{Si}_4$  layer (as identified by EBSD in Figure 2 c)). It remains unclear whether NW growth is occurring *via* a base or tip addition, however, the compositional homogeneity of the NWs would suggest that Cu diffusion occurs at the base rather than at the tip of the NW. The preference for growth of 1-D structures rather than continued bulk crystal formation has previously been linked to the existence of a time point in the reaction where the vapour supersaturation level decreases, such that anisotropic growth is favoured rather than addition to limited surface nucleation points.<sup>31,32,46-48</sup> In the context of the single injection protocol employed here, it is logical that bulk crystallite growth should occur at the initial stage of the reaction where the Si concentration is at its highest. As the silane is consumed by the reaction with the Cu foil, the supersaturation drops such that NW growth is favoured over continued bulk growth. As a result, the use of a single precursor introduction is a convenient means of attaining the supersaturation profile required for NW growth. This system may facilitate the growth of silicide NWs from alternative metals which are known to diffuse within Si (e.g. Fe,<sup>49</sup> Ti<sup>50</sup> and Cr<sup>51</sup>) which have not been grown by Si delivery to metal foils.

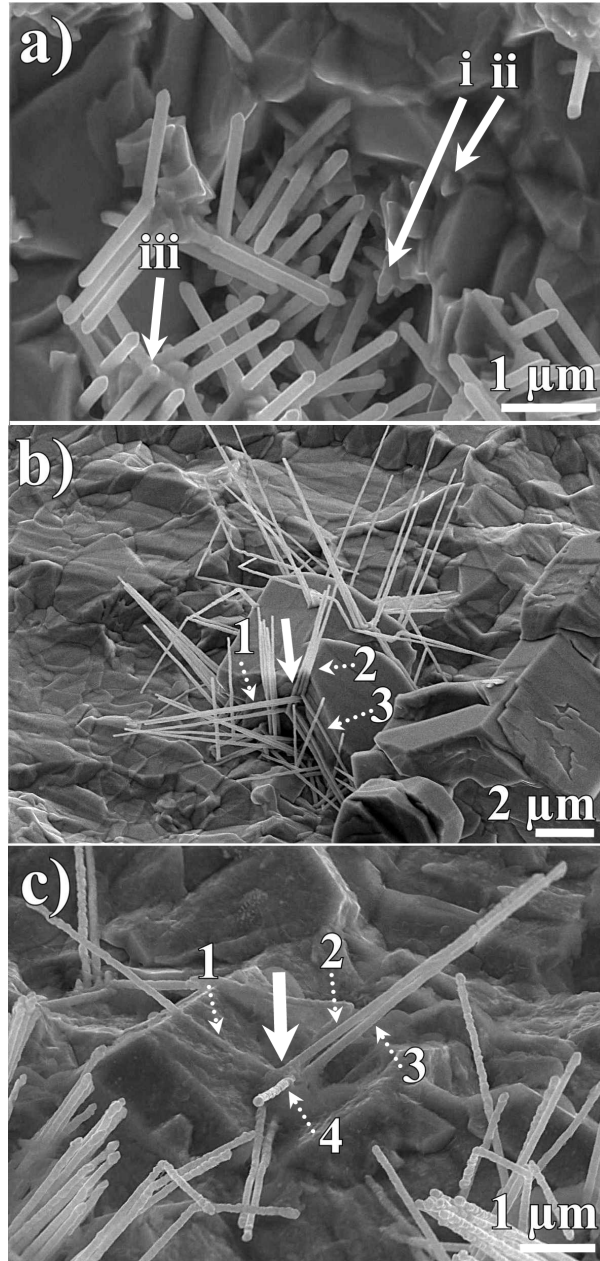


**Figure 4:** SEM images showing NW nucleation from the underlying substrate. a) 10 minute reaction showing short NWs and highlighted NW nucleation points (i,ii,ii). b) Low magnification image showing multiple NW nucleations from an individual crystallite. The area highlighted with the arrow shows the orientation of multiple NWs from one crystal facet. c) 4 highlighted NWs growing from the marked central crystallographic region.

To further examine the NW growth phenomenon, various nucleation points between NWs and underlying crystallites were examined (Figure 4). In Figure 4 a) the SEM image was taken from a ten minute reaction where NW growth was just beginning. A number of short ( $\approx 1 \mu\text{m}$  in length) NWs growing from the underlying crystallites can clearly be seen in the image. Additional nucleation points

which appear to be the starting points for NW growth from larger existing crystallites (marked in the image as i,ii) can also be seen. The nucleation of a NW from the intersection of two preformed NWs is marked as iii in the image and is consistent with the more complex geometrical NW structures previously highlighted. It appears that this NW segment is growing from a common central crystallographic region, which would be expected for the three and four fold geometries noted in this study. The role of the underlying material in determining the NW orientation can further be seen in Figure 4 b) where the majority of NWs in the image are growing from a single Cu silicide crystallite. The central region highlighted with the arrow is the nucleation point for NWs with three major orientations (1,2,3). Due to the 70 ° tilt of the sample during imaging, it is difficult to ascertain the precise angles of the NWs with relation to each other, however, NWs 1 and 3 can be seen to be near parallel to the major faces of the crystallite while the NWs marked 2 are growing vertically along the crystallite. The NW marked 1 in Figure 4 c) can be seen to grow along the surface of the underlying Cu silicide crystal (with the nucleation point highlighted with an arrow) with growth continuing to form a freestanding NW after it has grown past the edge of the crystallite. Thus, it appears that the underlying crystalline material determines the NW orientation both due to the crystallographic relationship and by physically constraining the NW growth (in the case of NWs growing along crystallite faces). In this context, it may be possible in future to define NW orientation and perhaps diameter by controlling the orientation and size of the Cu source (for example using patterned Cu substrates).

Figure 5 shows the  $I$ - $V$  curves from the  $\text{Cu}_{15}\text{Si}_4$  NWs deposited on a Au electrode (Fig. 5<sub>(1,2)</sub>). Two terminal transport measurements acquired between the contacts showed perfect ohmicity and differential conductance ( $dI/dV$ ) analysis (inset) shows no asymmetry in the curves confirming a purely ohmic transport through the NW. From  $I$ - $V$  analysis, the unit resistance was determined to be  $266 \, \Omega \, \mu\text{m}^{-1}$  with a corresponding resistivity  $\rho = \sim 208 \, \mu\Omega \, \text{cm}$  for a  $\text{Cu}_{15}\text{Si}_4$  NW with a  $\sim 100 \, \text{nm}$  diameter, circular cross-section. Additional information on the electrical analysis and an SEM image

of the device are presented in the Supporting Information (Figure S9 for the latter). The coupling capacitance was calculated at  $7.7 \text{ aF } \mu\text{m}^{-1}$  with an inductance of  $0.43 \text{ pH } \mu\text{m}^{-1}$ . The NWs presented here compare well with many other NW silicide interconnect alternatives in terms of resistivity (FeSi  $210 \text{ } \mu\Omega \text{ cm}$ ,<sup>52</sup>  $\text{Ti}_5\text{Si}_4$   $114 \text{ } \mu\Omega \text{ cm}$ ,<sup>53</sup>  $\text{TaSi}_2$   $210 \text{ } \mu\Omega \text{ cm}$ ,<sup>11</sup>  $\text{CoSi}$   $510 \text{ } \mu\Omega \text{ cm}$ ,<sup>54</sup>) but remain some way behind those noted for NiSi NWs ( $10 \text{ } \mu\Omega \text{ cm}$ )<sup>8</sup> and  $\text{CoSi}_2$  NWs ( $30 \text{ } \mu\Omega \text{ cm}$ ).<sup>55</sup> Further analysis will focus on effective current density carrying ability, carrier propagation speed and lower power dissipation, as these are the main requirements for a viable interconnect material.<sup>56</sup>

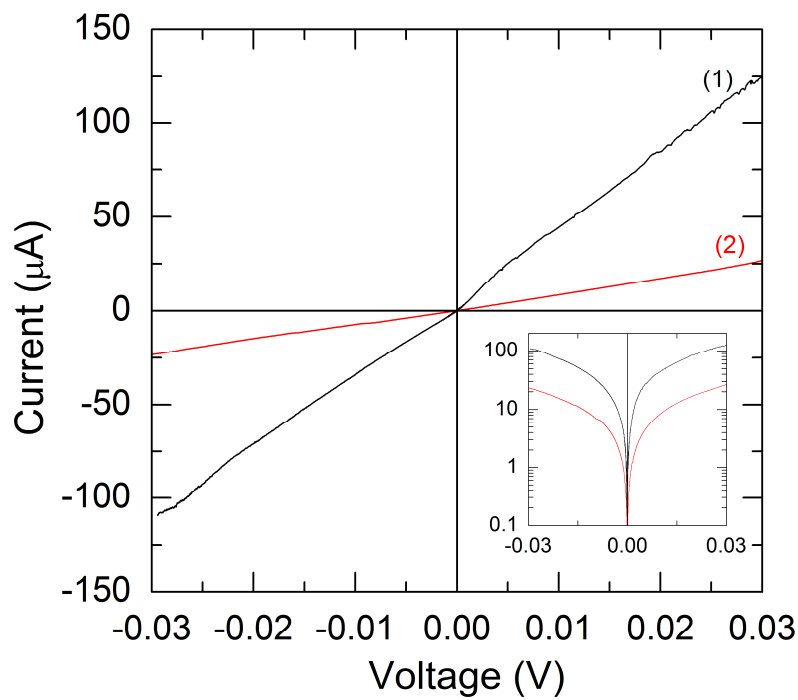


**Figure 5.** *I-V* curves of a 100 nm diameter  $\text{Cu}_{15}\text{Si}_4$  NW acquired using (1) four and (2) two terminal measurements.

**Conclusion:**

In conclusion, we report the high density growth of  $\text{Cu}_{15}\text{Si}_4$  NWs from bulk Cu foil in the vapour phase of a high boiling point solvent. The growth mechanism is dependent on the prior formation of  $\text{Cu}_{15}\text{Si}_4$  crystallites, from which the NWs nucleate. The orientation of the NWs from the underlying crystallites was examined, and it was found that the NWs possessed similar  $\langle 111 \rangle$  growth directions resulting in tetrahedral distributions of the arms giving densely packed tetrapod morphologies on the surface. The importance of Cu diffusion from the underlying substrate was illustrated by the transition of growth to silicide seeded Si NW formation instead of single crystal silicide NWs in copper poor conditions. The electrical properties of the NWs suggest promise for interconnect applications particularly given the material compatibility of copper and silicon for the semiconductor industry. Future work will concentrate on further reductions in wire diameters through size control of the emerging wire nuclei from the bulk crystals. Considering metal silicides NWs are an important emerging material set, the demonstrated ability to generate a new Cu silicide phase in NW form using glass-ware apparatus provides a highly attractive low cost and scalable synthetic protocol for advanced material development.

**Acknowledgements:**

This work was supported principally by Science Foundation Ireland (SFI) under the Principal Investigator Program under contract No. 06/IN.1/I85 and also by the Advanced Biomimetic Materials for Solar Energy Conversion Strategic Research Cluster (contract 07/SRC/B1160). This work was also conducted under the framework of the INSPIRE programme, funded by the Irish Government's Programme for Research in Third Level Institutions, Cycle 4, National Development Plan 2007–2013. Funding is acknowledged under the Irish Research Council for Science, Engineering and Technology (IRCSET) embark initiative for HG. HG would also like to acknowledge Dr. Fathima Laffir for XPS analysis and interpretation.

## Supporting information:

Additional details on electrical analysis and characterization is available in the supporting information.

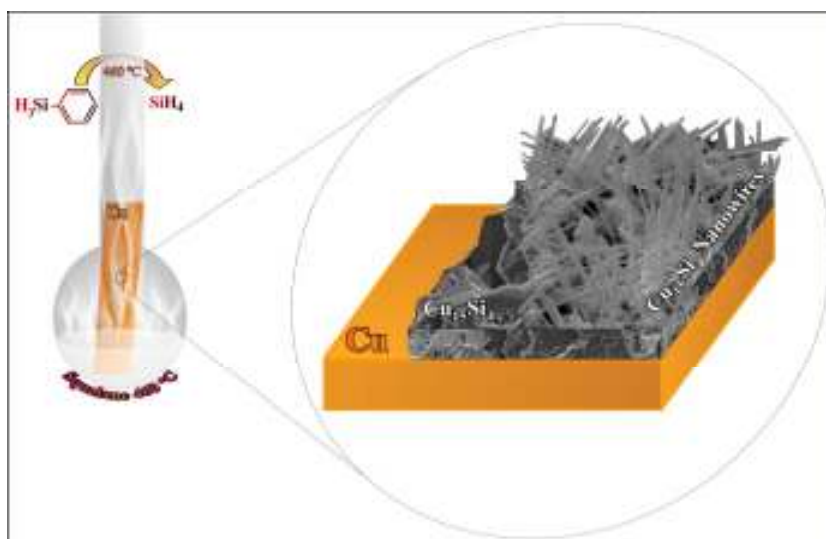
## References:

- (1) Schmitt, A. L.; Higgins, J. M.; Szczech, J. R.; Jin, S. *Journal of materials chemistry* **2010**, *20*, 223-235.
- (2) Kang, K.; Kim, S.-K.; Kim, C.-J.; Jo, M.-H. *Nano Letters* **2008**, *8*, 431-436.
- (3) Ouyang, L.; Thrall, E. S.; Deshmukh, M. M.; Park, H. *Advanced Materials* **2006**, *18*, 1437-1440.
- (4) Chou, Y.-C.; Wu, W.-W.; Cheng, S.-L.; Yoo, B.-Y.; Myung, N.; Chen, L. J.; Tu, K. N. *Nano Letters* **2008**, *8*, 2194-2199.
- (5) Lee, C.-Y.; Lu, M.-P.; Liao, K.-F.; Lee, W.-F.; Huang, C.-T.; Chen, S.-Y.; Chen, L.-J. *The Journal of Physical Chemistry C* **2009**, *113*, 2286-2289.
- (6) Lu, K.-C.; Wu, W.-W.; Wu, H.-W.; Tanner, C. M.; Chang, J. P.; Chen, L. J.; Tu, K. N. *Nano Letters* **2007**, *7*, 2389-2394.
- (7) Kim, J.; Shin, D. H.; Lee, E. S.; Han, C. S.; Park, Y. C. *Applied Physics Letters* **2007**, *90*.
- (8) Wu, Y.; Xiang, J.; Yang, C.; Lu, W.; Lieber, C. M. *Nature* **2004**, *430*, 61-65.
- (9) Zhou, S.; Liu, X.; Lin, Y.; Wang, D. *Angewandte Chemie International Edition* **2008**, *47*, 7681-7684.
- (10) Szczech, J. R.; Schmitt, A. L.; Bierman, M. J.; Jin, S. *Chemistry of Materials* **2007**, *19*, 3238-3243.
- (11) Chueh, Y.-L.; Ko, M.-T.; Chou, L.-J.; Chen, L.-J.; Wu, C.-S.; Chen, C.-D. *Nano Letters* **2006**, *6*, 1637-1644.
- (12) Liu, Z.; Zhang, H.; Wang, L.; Yang, D. *Nanotechnology* **2008**, *19*, 375602.
- (13) Barrett, C. A.; Gunning, R. D.; Hantschel, T.; Arstila, K.; O'Sullivan, C.; Geaney, H.; Ryan, K. M. *Journal of materials chemistry* **2010**, *20*, 135-144.
- (14) Hymes, S.; Kumar, K. S.; Murarka, S. P.; Ding, P. J.; Wang, W.; Lanford, W. A. *Journal of Applied Physics* **1998**, *83*, 4507-4512.
- (15) Parajuli, O.; Kumar, N.; Kipp, D.; Hahm, J. I. *Applied Physics Letters* **2007**, *90*.
- (16) Li, S.; Cai, H.; Gan, C. L.; Guo, J.; Dong, Z.; Ma, J. *Crystal Growth & Design* **2010**, *10*, 2983-2989.
- (17) Zhang, Z.; Wong, L. M.; Ong, H. G.; Wang, X. J.; Wang, J. L.; Wang, S. J.; Chen, H.; Wu, T. *Nano Letters* **2008**, *8*, 3205-3210.
- (18) Jung, S. J.; Lutz, T.; Bell, A. P.; McCarthy, E. K.; Boland, J. J. *Crystal Growth & Design* **2012**.
- (19) Wu, W.; Yu, Q. K.; Zhang, J. M.; Lian, J.; Liang, G.; Ewing, R. C.; Pei, S. S. *Applied Physics Letters* **2008**, *92*, 3.
- (20) Ng, P. K.; Fisher, B.; Low, K. B.; Joshi-Imre, A.; Bode, M.; Lilley, C. M. *Journal of Applied Physics* **2012**, *111*, 104301-7.

- (21) Geaney, H.; Kennedy, T.; Dickinson, C.; Mullane, E.; Singh, A.; Laffir, F.; Ryan, K. M. *Chemistry of Materials* **2012**.
- (22) Tuan, H.-Y.; Korgel, B. A. *Chemistry of Materials* **2008**, *20*, 1239-1241.
- (23) Barrett, C. A.; Geaney, H.; Gunning, R. D.; Laffir, F. R.; Ryan, K. M. *Chemical Communications* **2011**, *47*, 3843-3845.
- (24) Geaney, H.; Dickinson, C.; Barrett, C. A.; Ryan, K. M. *Chemistry of Materials* **2011**, *23*, 4838-4843.
- (25) Geaney, H.; Dickinson, C.; Weng, W.; Kiely, C. J.; Barrett, C. A.; Gunning, R. D.; Ryan, K. M. *Crystal Growth & Design* **2011**, *11*, 3266-3272.
- (26) Mullane, E.; Geaney, H.; Ryan, K. M. *Chemical Communications* **2012**, *48*, 5446-5448.
- (27) Leung, Y.; Kwok, W.; Djurić, A.; Phillips, D.; Chan, W. *Nanotechnology* **2005**, *16*, 579.
- (28) Milliron, D. J.; Hughes, S. M.; Cui, Y.; Manna, L.; Li, J.; Wang, L.-W.; Paul Alivisatos, A. *Nature* **2004**, *430*, 190-195.
- (29) Manna, L.; Scher, E. C.; Alivisatos, A. P. *Journal of the American Chemical Society* **2000**, *122*, 12700-12706.
- (30) Okamoto, H. *Journal of Phase Equilibria* **2002**, *23*, 281-282.
- (31) Kim, C. J.; Kang, K.; Woo, Y. S.; Ryu, K. G.; Moon, H.; Kim, J. M.; Zang, D. S.; Jo, M. H. *Advanced Materials* **2007**, *19*, 3637-3642.
- (32) Liu, Z. H.; Zhang, H.; Wang, L.; Yang, D. R. *Nanotechnology* **2008**, *19*.
- (33) Yan, X.; Yuan, H.; Wang, J.; Liu, D.; Zhou, Z.; Gao, Y.; Song, L.; Liu, L.; Zhou, W.; Wang, G. *Applied Physics A: Materials Science & Processing* **2004**, *79*, 1853-1856.
- (34) Hymes, S.; Kumar, K.; Murarka, S.; Ding, P.; Wang, W.; Lanford, W. *J. Appl. Phys.* **1998**, *83*, 4507.
- (35) Chromik, R. R.; Neils, W. K.; Cotts, E. J. *Journal of Applied Physics* **1999**, *86*, 4273-4281.
- (36) Renard, V. T.; Jublot, M.; Gergaud, P.; Cherns, P.; Rouchon, D.; Chabli, A.; Jousseume, V. *Nat Nano* **2009**, *4*, 654-657.
- (37) Wen, C. Y.; Reuter, M. C.; Tersoff, J.; Stach, E. A.; Ross, F. M. *Nano Letters* **2009**, *10*, 514-519.
- (38) Arbiol, J.; Kalache, B.; Cabarrocas, P. R. i.; Morante, J. R.; Morral, A. F. i. *Nanotechnology* **2007**, *18*, 305606.
- (39) Singh, A.; Dickinson, C.; Ryan, K. M. *ACS Nano* **2012**, *6*, 3339-3345.
- (40) Chen, X.; Kim, M. H.; Zhang, X.; Larson, C.; Yu, D.; Wodtke, A. M.; Moskovits, M. *The Journal of Physical Chemistry C* **2008**, *112*, 13797-13800.
- (41) Bomben, K. D.; Chastain, J.; Moulder, J.; Sobol, P.; Stickle, W. *Perkin-Elmer Corporation, Physical Electronics Division* **1992**.
- (42) Sarkar, D. K.; Bera, S.; Narasimhan, S. V.; Chowdhury, S.; Gupta, A.; Nair, K. G. M. *Solid State Communications* **1998**, *107*, 413-416.
- (43) Shin, D.-W.; Wang, S. X.; Marshall, A. F.; Kimura, W.; Dong, C.; Augustsson, A.; Guo, J. *Thin Solid Films* **2005**, *473*, 267-271.
- (44) Wen, C. Y.; Reuter, M. C.; Tersoff, J.; Stach, E. A.; Ross, F. M. *Nano Letters* **2010**, *10*, 514-519.
- (45) Venables, J. A.; Spiller, G. D. T.; Hanbucken, M. *Reports on Progress in Physics* **1984**, *47*, 399-459.

- (46) Xia, Y.; Yang, P.; Sun, Y.; Wu, Y.; Mayers, B.; Gates, B.; Yin, Y.; Kim, F.; Yan, H. *Advanced Materials* **2003**, *15*, 353-389.
- (47) Guiton, B. S.; Gu, Q.; Prieto, A. L.; Gudiksen, M. S.; Park, H. *Journal of the American Chemical Society* **2004**, *127*, 498-499.
- (48) Pan, Z. W.; Dai, Z. R.; Wang, Z. L. *Science* **2001**, *291*, 1947.
- (49) Struthers, J. *Journal of Applied Physics* **1956**, *27*, 1560.
- (50) Hocine, S.; Mathiot, D. *Applied Physics Letters* **1988**, *53*, 1269-1271.
- (51) Conzelmann, H.; Graff, K.; Weber, E. *Applied Physics A: Materials Science & Processing* **1983**, *30*, 169-175.
- (52) Schmitt, A. L.; Bierman, M. J.; Schmeisser, D.; Himpsel, F. J.; Jin, S. *Nano Letters* **2006**, *6*, 1617-1621.
- (53) Chang, C.-M.; Chang, Y.-C.; Lee, C.-Y.; Yeh, P.-H.; Lee, W.-F.; Chen, L.-J. *The Journal of Physical Chemistry C* **2009**, *113*, 9153-9156.
- (54) Schmitt, A. L.; Zhu, L.; Schmeißer, D.; Himpsel, F. J.; Jin, S. *The Journal of Physical Chemistry B* **2006**, *110*, 18142-18146.
- (55) Okino, H.; Matsuda, I.; Hobara, R.; Hosomura, Y.; Hasegawa, S.; Bennett, P. A. *Applied Physics Letters* **2005**, *86*, 3.
- (56) Morimoto, T.; Ohguro, T.; Momose, H. S.; Iinuma, T.; Kunishima, I.; Suguro, K.; Katakabe, I.; Nakajima, H.; Tsuchiaki, M.; Ono, M.; Katsumata, Y.; Iwai, H. *Ieee Transactions on Electron Devices* **1995**, *42*, 915-922.

#### TOC graphic:



Here, we report the formation of high density arrays of  $\text{Cu}_{15}\text{Si}_4$  nanowires using a high boiling point organic solvent based method. The reactions were carried out using Cu foil substrates as the Cu source with nanowire growth dependent upon the prior formation of  $\text{Cu}_{15}\text{Si}_4$  crystallites on the surface. The wires grow from the underlying [111] facets of the bulk crystals resulting in a tetrahedral angular distribution of wire arrays with multiple wires emerging from each facet. The method shows that simple Si delivery to metal foil can be used to grow high densities of silicide nanowires with a tight diameter spread at reaction temperatures of 460 °C. The nanowires are characterized by HRTEM, HRSEM, XPS and show low resistivities, while coupling capacity and unit impedance were also determined through electrical analysis.